Microseism and infrasound generation by cyclones

Samuel P. Bowen and Jacques C. Richard
Chicago State University, Chicago, Illinois 60628

Jay D. Mancini, Vassilios Fessatidis, and Benjamin Crooker
Fordham University, Bronx, New York 10458

(Received 3 July 2001; revised 12 February 2003; accepted 19 February 2003)

A two-dimensional cylindrical shear-flow wave theory for the generation of microseisms and infrasound by hurricanes and cyclones is developed as a linearized theory paralleling the seminal work by Longuet-Higgins which was limited to one-dimensional plane waves. Both theories are based on Bernoulli's principle. A little appreciated consequence of the Bernoulli principle is that surface gravity waves induce a time dependent pressure on the sea floor through a vertical column of water. A significant difference exists between microseisms detected at the bottom of each column and seismic signals radiated into the crust through coherence over a region of the sea floor. The dominant measured frequency of radiated microseisms is matched by this new theory for seismic data gathered at the Fordham Seismic Station both for a hurricane and a mid-latitude cyclone in 1998. Implications for Bernoulli's principle and this cylindrical stress flow theory on observations in the literature are also discussed.
[DOI: 10.1121/1.1567277]

PACS numbers: 43.30.Nb, 43.28.Dm, 43.28.Hr, 43.40.Ph [SAC-B]

I. INTRODUCTION

The phenomena of storm-generated microseisms, the low frequency and low intensity seismic signals recorded on land-based seismometers that are associated with storms moving across water, has been observed by many scientists over the years. A very thorough review of such ''radiated'' microseisms and the related infrasound effects has been written by Tabulevich[1] and contains qualitative data that offers insights into the causes of microseisms. Through many years of observations, Tabulevich and colleagues observed that microseisms were closely associated with moving cyclones passing over water and that the cyclonic nature of the storm was essential, there being no significant microseisms associated with linear wave fronts. She conducted triangulation studies to locate the sources of microseisms and identified specific storms as had others. For example, as early as 1940, Ramirez[2] used three seismographs to triangulate cyclones using microseismic signals. More recently, other observers[3] using arrays of seismometers have closely associated microseisms with strong cyclonic storms at sea.

The study reported in this paper was carried out to collect detailed data on large cyclones, both hurricanes and mid-latitude cyclones, in order to test various theories predicting the dominant microseism frequency and other properties of the observed ''radiated'' microseisms as detected by land-based seismometers. While developing the new theory it became clear that certain distinctions between radiated microseisms and sea floor detected microseisms needed to be clarified. While the cyclone data and theory are the main focus of this paper, some attention will be paid to these distinctions.

The foundational theoretical study of the radiation of microseisms from the sea floor to land-based seismometers was carried out by Longuet-Higgins[4] (LH), who used Bernoulli's principle, linearized hydrodynamic equations and one-dimensional plane waves moving across the surface of the water to explore possible mechanisms by which microseisms could be generated. One of the first important questions that LH addressed was the apparent contradiction between the fact that surface gravity waves are restricted to a narrow region near the surface and the evidence that pressures at the sea floor are an essential part of microseism generation. How could waves restricted to the surface have an impact on the sea floor pressures? There are essentially two different mechanisms that resolve this apparent contradiction. The first mechanism is the application of the Bernoulli principle to each vertical column of water connecting the surface to the sea floor. Bernoulli's principle states that the sum of the pressure, the kinetic energy per unit volume, and the potential energy per unit volume must have the same value at all points in the column, even if any of these variables are varying in time. The immediate consequence of this is that the pressure time dependence at the base of a column of water is determined by the time dependence of the surface gravity waves at the top of the column, and this effect is independent of the depth. The second mechanism,[5] to be discussed below, is the generation of acoustic waves through the nonlinear interaction of surface gravity waves. The resulting acoustic waves are not damped with depth and their propagation down to the sea floor provides a generation mechanism for microseisms.

LH's most often quoted result is the observation that a standing wave is the only one-dimensional plane wave structure which can generate radiated microseisms. In most of the literature, it has not been widely appreciated that this part of LH's analysis applies only to the radiation of seismic signals through the earth's crust to distant seismographs. As is discussed below, Bernoulli's principle alone is adequate to generate microseisms detected at a fixed sea bottom location. Also the generation of a seismic signal radiating into the

 0001-4966/2003/113(5)/2562/12/$19.00

crust and scaling with the size of the storm requires a wave with spatial coherence and persistence.

LH also observed that Bernoulli's principle implies that the kinetic energy of the surface wave gives rise to pressure fluctuations on the sea floor, which will be observed at twice the frequency of the surface wave. This $2f$ signal is a direct consequence of Bernoulli's principle and expresses a nonlinearity in the sense that the square of the velocity in the kinetic energy produces the effect on the pressure. The $2f$ signal is not exclusively a sign that nonlinear interactions between surface gravity waves are involved in the production of that signal.

In contrast to the studies by Tabulevich which are interpreted exclusively through Bernoulli's principle, a prominent school of thought has focused on the generation of acoustic waves by nonlinear interactions between surface gravity waves. From this perspective, microseisms are caused by the acoustic waves which are not damped with depth under the surface. The chief proponent of this effect has been Kibblewhite who has developed mechanisms for producing these acoustic waves in great detail.[6] The initial motivation for the consideration of these nonlinear effects was a hydrophone study by Nichols,[7] who concluded that nonlinear mechanisms must be involved since the $2f$ peak was so prominent. It is worth noting that Nichols included LH's work as part of this nonlinear theory and did not definitively distinguish between the two generation mechanisms listed above. Kibblewhite and colleagues[6] have worked out a number of details of the generation and consequences of acoustic waves generating microseisms. The dominant gravity waves that are assumed to be involved in microseism generation are pairs of waves moving in almost opposite directions.

The decisive researcher in this school has been Webb, who has conducted a number of exceptionally well-crafted experiments with carefully gathered data to probe the fine structure of a wide variety of theories. He collected sea-floor microseism data[8] at several depths and sites in the Pacific. Much of this data represented the microseisms generated by the ''equilibrium'' wave distribution above the detector, but some interesting data was collected for what appears to be a mid-latitude cyclone which passed near the site. He also collected fascinating data on microseisms under the frozen ice pack in the Beaufort Sea.[9] This very quiet data offers further data to distinguish between competing theories. Finally, he explored the interesting idea of the ''climatology'' [10] of bottom detected microseisms by seeking to predict the microseism spectrum from the wave height distribution associated with the surface. While these data are not central to the present work, a brief discussion of several of these measurements from the point of view of the Bernoulli principle is presented at the end of this paper.

The Longuet-Higgins conclusion about standing waves has been part of the guiding foundation for experiments on microseisms over the years since his paper. Because a standing wave can be obtained from the linear combination of two oppositely traveling waves with equal amplitudes, several observers sought to find standing waves caused by reflections from shore emplacements, harbors, and partially enclosed bodies of water. The equality of amplitudes is essential for the formation of a standing wave. In few of these cases was consideration made of the possible change in amplitude from various reflections considered. Tabulevich among others attempted to have the wind waves ahead of a moving cyclone and those which follow the storm, and move in opposite directions, combining to form standing waves, even when these two winds were not present at the same point at the same time. Other discussions have associated standing waves with wind direction changes and cross winds.[8] Detailed measurements by Kibblewhite and Ewans[11] at the Maui Development site were also interpreted as being caused by waves running into a recently changing wind and thus possibly encountering oppositely moving waves of similar amplitude. In general, searches for one dimensional, plane, standing waves as a cause of microseisms have been inferential, that is, mostly without direct observations. Careful, well-instrumented shallow ocean bottom observations[12] found no evidence of standing waves, or even significant reflected waves from nearby shores. On the other hand, several studies with under water pressure detectors and seismometers observed microseisms in the presence of swell[13] from far away storms and shore, wind,[8] and what would be expected to be predominantly traveling waves.

This paper is presented in the conviction that all of the consequences of the linear theory based on Bernoulli's principle need to be more deeply examined, and that there exists a wave form, other than one-dimensional, plane standing waves, not considered by LH, that can give rise to microseisms. In particular, cylindrical waves on the two-dimensional air–fluid interface around the center of a cyclone can also generate microseisms and rationalize much of the existing data in the literature. The role of the wind and the cyclonic nature of the storms associated with microseisms is explored below.

In the following sections, the LH study for one-dimensional plane waves on the surface and its relationship to microseism development is reviewed. Emphasis will be given to the difference between stationary bottom measurements and extensive coherent area sources for radiated microseisms. Briefly discussed are two different approaches to microseism generation which parallel the wind generation of water waves,[14] namely, the resonance theory of Phillips[15] and the shear flow theory of Miles.[16] A resonance theory of microseism generation is found to agree with the LH traveling wave null results in the absence of viscosity, but does predict a double frequency peak whose amplitude is probably too small to be observed in land-based seismometers. A two-dimensional theory, the cyclonic shear flow theory, is developed that exhibits double frequency peaks in the microseism spectra, the frequency of which depends on the cylindrical velocity structure of the atmospheric storm and the associated flow in the water. This theory will be applied to two different kinds of cyclonic storms: tropical hurricanes which are represented by a vortex line with an eye wall, centered on the storm, and mid-latitude cyclones which have almost circular isobars and a constant radial pressure gradient about their center. This shear flow theory is compared to land-based seismic measurements of two different storms in 1998: a Nor'easter in January and Hurricane Bonnie in August. Good success is achieved in predicting the frequency of the double frequency peak from first principles and several other features of Bonnie. In the last section, consequences of these ideas are applied to observations of Tabulevich, Kibblewhite, and Ewans, and climatology of microseisms, and sea-floor spectral measurements of Webb.

II. REVIEW OF GOVERNING EQUATIONS FOR INCOMPRESSIBLE FLUIDS

In this section the notation and background for gravity waves is established. The beginning is the Navier–Stokes equation for the force on a mass of material of density ρ and velocity u. Following Mei,[17] yields the momentum equation of motion:

$$\frac{\partial u}{\partial t}+u\cdot\nabla u=-\nabla\left(\frac{P}{\rho}+gz\right)+\nu\nabla^2 u, \tag{1}$$

where ν is the constant kinematic viscosity, P is the pressure, and g is the local acceleration of gravity, and the z axis is pointing upward. When the flow is laminar and the viscosity is small, a velocity potential Φ approximately determines the velocity u through

$$u=\nabla\Phi. \tag{2}$$

Substituting into the Navier–Stokes equation yields for Φ the following equation:

$$\nabla\left(\frac{\partial\Phi}{\partial t}+\frac{1}{2}|\nabla\Phi|^2-\nu\nabla^2\Phi\right)=-\nabla\left(\frac{P}{\rho}+gz\right). \tag{3}$$

Without the viscosity this equation leads to the Bernoulli principle that

$$\frac{\partial\Phi}{\partial t}+\frac{1}{2}|\nabla\Phi|^2+\frac{P}{\rho}+gz=C(t), \tag{4}$$

where $C(t)$ is a constant in space, dependent only, possibly on time. Because $C(t)$ does not depend on depth, the pressure at the sea floor (the coordinate system has the unperturbed surface at $z=0$ and the sea floor at $z=-h$), where $\nabla\Phi$, $\partial\Phi/\partial t\rightarrow 0$ as $z\rightarrow -h$,

$$\frac{\partial\Phi}{\partial t}+\frac{1}{2}|\nabla\Phi|^2+\frac{P(0)}{\rho}+gz=\frac{P(-h)}{\rho}-gh. \tag{5}$$

In the following discussion the continuity equation and the boundary conditions are written for the surface and bottom of the body of water, assuming that all quantities have a $e^{-i\omega t}$ time dependence. Viscous effects are kept to lowest order where necessary, but the $|\nabla\Phi|^2$ terms are neglected.

Given that the coordinate system has the unperturbed surface at $z=0$ and the sea floor at $z=-h$, the equation of continuity for the velocity potential is

$$\nabla^2\Phi=0,\quad -h<z<0. \tag{6}$$

The velocity at the sea floor must vanish so the following condition on the normal derivative of the velocity potential must hold:

$$\frac{\partial\Phi}{\partial n}=0,\quad z=-h. \tag{7}$$

The kinematic boundary condition at the free surface is that the changes in the surface are caused by the velocity field of the fluid, so the time rate of change of the surface position must be equal to the speed of the fluid in the vertical direction:[17]

$$\frac{\partial\eta}{\partial t}=\frac{\partial\Phi}{\partial z},\quad z=0. \tag{8}$$

Combining this surface boundary condition with the equation of motion for Φ yields the equivalent of a wave equation at the surface,

$$\frac{\partial^2\Phi}{\partial t^2}+g\frac{\partial\Phi}{\partial z}-\nu\nabla^2\frac{\partial\Phi}{\partial t}=-\frac{1}{\rho}\frac{\partial P_a}{\partial t},\quad z=0. \tag{9}$$

Assuming that the surface of the water bears a wave with wave vector k, $\eta=Ae^{ikx}$ yields the following dispersion relation for gravity waves propagating along the surface:

$$\omega(k)^2=gk\tanh(kh), \tag{10}$$

and these waves are damped exponentially with depth.

As with any physical system it is expected that if an atmospheric pressure disturbance with a velocity v matching the gravity wave phase velocity for some wave vector k,

$$v=\sqrt{\frac{g\tanh(kh)}{k}}=\frac{\omega(k)}{k}, \tag{11}$$

there should be some sort of resonant interaction.

Precisely this resonant effect has been considered by Phillips[15] in the study of transient wave development in the ocean.[14]

III. REVIEW OF THE LONGUET-HIGGINS STUDY

The excitation of gravity waves in the linearized theory above for an incompressible fluid is localized to within a few wavelengths of the surface since the waves are damped out with increasing depth. However, the time dependence of the surface gravity waves can be transmitted to the ocean floor through the column of water between the surface and the floor via the Bernoulli principle. For laminar flow this principle relates the atmospheric pressure at the surface P_a to the pressure $P(x,y,-h)$ at a depth h on the floor

$$P_a+\rho g\eta(x,y,t)+\tfrac{1}{2}\rho v(x,y,\eta,t)^2=P(x,y,-h)-\rho gh, \tag{12}$$

where $v(x,y,\eta,t)$ is the velocity of the surface waves at the surface point (x,y), $\eta(x,y,t)$ is the water surface profile about $z=0$, ρ is the density of the water, g is the local acceleration of gravity, and it is assumed that the bottom velocity of the water is zero. From this principle the pressure at a point $(x,y,-h)$ on the bottom should show the time dependence of the surface gravity waves

$$P(x,y,-h)=P_a+\rho g(h+\eta(x,y,t))+\tfrac{1}{2}\rho v(x,y,\eta,t)^2. \tag{13}$$

Consider as a simple example, a vertically oriented traveling wave with wave vector k and angular frequency ω,

$$\eta(x,y,t)=A\sin(kx-\omega t), \tag{14}$$

$$v(x,y,0,t)=\omega A\cos(kx-\omega t). \quad (15)$$

The bottom pressure at a fixed position $(x,y,-h)$ will have the following time dependences:

$$P(x,y,-h)=P_a+\rho g(h+A\sin(kx-\omega t)) + \tfrac{1}{2}\rho\omega^2A^2\cos(kx-\omega t)^2. \quad (16)$$

Thus, if a single frequency traveling wave from some source, like a hurricane or typhoon, passes over a point x, this simple traveling wave would generate a pressure power spectrum with peaks at ω and 2ω. Such observations have clearly been made with the bottom placed seismic and pressure observations of Sutton and Barstow.[13]

The Longuet-Higgins well-known conditions about standing waves being necessary for surface radiated microseisms are not applicable to signals received at a single point on the bottom. The measurements and observations of this paper and the LH original study deal with the radiation of seismic signals from the ocean floor and their propagation through the surface and body of the earth to a distant seismometer. This distinction is clarified in the following paragraphs.

Longuet-Higgins began his study by looking at the generation of seismic waves by a source induced on the floor of the ocean. For simplicity, in the following discussion, an approximate Green's function for the propagation of the seismic signal through the surface of the earth will be used instead of a more detailed Green's function that reflects the surface boundary conditions and curvature of the earth. The more complete Green's function shares the property of depending on coherence in the source region for signal propagation so our arguments below will remain valid for the more accurate formulas.

For simplicity, assume a storm occupies surface over a rectangular sea-floor section of length L and width W with an area $L\times W$, which region is a distance R from the seismometer, then the vertical displacement $\mathbf{s}$ of the seismometer at a frequency ω is given approximately in the far field region[18] by

$$\mathbf{s}(R,\omega)=\frac{e^{i(\omega/c_s)R}}{c_s^2\rho_s R}W\int_0^L P(x,y,-h,\omega)\,dx, \quad (17)$$

where c_s is the velocity of sound in the earth's crust, ρ_s is an average density of the solid in the crust, and for the following examples it will be assumed that all plane waves are traveling along the x direction and there is no other dependence perpendicular to the x axis. This assumption reduces a surface integral over the area to the linear integral multiplied by W.

The primary assumption of Longuet-Higgins was that detectable radiated seismic signals are those in which the integral of the bottom pressure over an area is proportional to that area. To borrow language from thermodynamics, the signal has to be extensive in the area and energy of the storm. In our explicitly simplified example, the pressure integral should be proportional to L.

Examining the effect of the gravitational potential energy term on this region, shows that

$$\rho g W\int_0^L \sin(kx-\omega t)\,dx=\frac{\rho g}{k}W(\sin(kL-\omega t)+\sin(\omega t)), \quad (18)$$

which is not proportional to the area, vanishes (as noted by LH) whenever kL is a multiple of 2π, and will thus not scale with the size of the storm unless $k=0$, i.e., a stationary wave.

A similar observation can be found for the kinetic energy from the traveling surface gravity waves,

$$\int_0^L \rho v^2\,dx=W\frac{1}{2}\rho\omega^2A^2\frac{1}{k}(\cos(kL-\omega t)\sin(kL-\omega t) +\cos(\omega t)\sin(\omega t)+kL). \quad (19)$$

The time-dependent contribution for this one-dimensional plane traveling wave is not of order L unless $k=0$, as before.

Longuet-Higgins then asked whether there was any form of one-dimensional plane wave which would, through the kinetic energy, exert a force on the whole area and thus produce a detectable signal. In a straightforward manner he showed that a standing plane wave could produce a signal on the ocean floor that would scale with the area of the storm. The vertical velocity due to such a standing wave is given by

$$v=\omega A\cos(kx)\cos(\omega t), \quad (20)$$

and the kinetic energy integral has a positive integrand $\cos(kx)^2$ and becomes

$$\int_0^L \rho v^2\,dx=W\frac{1}{2}\rho\omega^2A^2\frac{1}{k} \times(\cos(kL)\sin(kL)+kL)\cos^2(\omega t), \quad (21)$$

which has an extensive, time-dependent contribution to the pressure at twice the wave frequency.

The current study began by asking if there is another type of wave disturbance on the surface which would give rise to an extensive force on the floor of the ocean. The search led to the examination of the two extreme types of theories for the generation of surface waves following the work of Phillips and Miles, and to examine two-dimensional cylindrical waves that are generated under wind fields of both the tropical hurricane and the mid-latitude cyclone.

IV. WAVE RESPONSE TO ATMOSPHERIC PRESSURE PROFILE: RESONANCE THEORY

If a large storm with its attendant pressure profile $P(x-vt)$ is moving through a region, Phillips'[19] resonance theory of wave excitation argues that those waves whose phase velocity is the same as the moving storm will be strongly excited. This resonance condition of matching the phase velocity selects a dominant wave vector satisfying the following equation.

$$kv=\omega(k). \quad (22)$$

Evaluating this condition for $\omega(k)=\sqrt{gk}$, valid for deep water, yields

$$\omega_v=vq=\omega(q)=\frac{g}{v} \quad (23)$$

and

$$q=\frac{g}{v^2}. \tag{24}$$

The resonance theory thus predicts a microseism frequency that is strongly dependent on the velocity of the storm.

A fairly straightforward calculation, in the limit of vanishing viscosity, yields the following for one of the surface wave velocities:

$$U=\frac{g\tilde{P}\left(\frac{g}{v^2}\right)}{2\rho v^2}\sin\left(\frac{g}{v}\left(t-\frac{x}{v}\right)\right), \tag{25}$$

where $\tilde{P}(g/v^2)$ is the spatial Fourier transform of the moving pressure profile $P(x)$. Note, however, that this is a traveling wave and hence does not contribute to distant seismometer signals (a consequence of the LH theorem for traveling waves).

Including the viscosity to lowest order in this resonance theory does give rise to a small peak at twice the resonance frequency, but its magnitude is proportional to the viscosity of the water and thus the signal would be very small.

There is another major problem with the resonance theory. It predicts that the frequency generated by a storm will become very large as the velocity of the storm approaches zero. As is discussed below, the hurricane Bonnie stopped or slowed considerably three times in its lifetime, twice at sea and once while it reversed directions at the Carolina coast and returned to sea. The dominant frequency of Bonnie's microseismic power spectrum is almost constant, velocity independent and does not obey this velocity dependence g/v_s. This flatly contradicts the resonance model.

V. GENERATION OF MICROSEISMS BY A SLOWLY MOVING HURRICANE: CYLINDRICAL SHEAR FLOW THEORY

In this section a theory is derived in which the atmospheric winds around a cyclone excite resonant excitations of the surface gravitational waves.

The treatment of the problem is in cylindrical coordinates with the quiescent surface of the sea at $z=0$. White[20] in his book on viscous flow discusses a classical cylindrical problem that had been earlier analyzed by von Karman.[21] This problem involved the flow of fluid near a infinite rotating disk with a no-slip boundary condition between the disk and fluid. The fluid velocity is expressed in terms of the cylindrical components

$$\mathbf{v}=v_r\mathbf{e}_r+v_\varphi\mathbf{e}_\varphi+v_z\mathbf{e}_z, \tag{26}$$

where the unit vectors $\mathbf{e}_r, \mathbf{e}_\varphi, \mathbf{e}_z$ form the standard orthonormal basis for cylindrical coordinates. Because of the expected cylindrical symmetry, these three velocity components and the pressure should be independent of φ, the azimuthal angle.

The governing equations include, the continuity equation

$$\frac{1}{r}\frac{\partial(rv_r)}{\partial r}+\frac{\partial v_z}{\partial r}=0, \tag{27}$$

the radial component of the momentum equation

$$\frac{\partial v_r}{\partial t}+v_r\frac{\partial v_r}{\partial r}+v_z\frac{\partial v_r}{\partial z}-\frac{v_\varphi^2}{r} =-\frac{1}{\rho}\frac{\partial p}{\partial r}+\nu\left(\frac{\partial^2 v_r}{\partial r^2}+\frac{1}{r}\frac{\partial v_r}{\partial r}+\frac{\partial^2 v_r}{\partial z^2}-\frac{v_r^2}{r}\right), \tag{28}$$

the azimuthal component of the momentum equation

$$\frac{\partial v_\varphi}{\partial t}+v_r\frac{\partial v_\varphi}{\partial r}+v_z\frac{\partial v_\varphi}{\partial z}-\frac{v_r v_\varphi}{r} =\nu\left(\frac{\partial^2 v_\varphi}{\partial r^2}+\frac{1}{r}\frac{\partial v_\varphi}{\partial r}+\frac{\partial^2 v_\varphi}{\partial z^2}-\frac{v_\varphi^2}{r}\right), \tag{29}$$

and the axial component of the momentum equation

$$\frac{\partial v_z}{\partial t}+v_r\frac{\partial v_z}{\partial r}+v_z\frac{\partial v_z}{\partial z} =-\frac{1}{\rho}\frac{\partial p}{\partial z}+\nu\left(\frac{\partial^2 v_z}{\partial r^2}+\frac{1}{r}\frac{\partial v_z}{\partial r}+\frac{\partial^2 v_z}{\partial z^2}\right). \tag{30}$$

For von Karmen's study, the boundary conditions were no slip at the disk and no viscous effects far from the disk except azimuthal flow, i.e., at $z=0$, $v_r=v_z=0$, $v_\varphi=r\Omega$, $p=0$, and as $z\to\infty$, $v_r=v_\varphi=0$. For this infinite rotating disk problem, von Karman deduced that the components v_r/r, v_φ/r, v_z, and p are all functions of z alone and was able to reduce this problem to one of the coupled ordinary differential equations, which he solved numerically.

The problem being studied here is very similar. A large storm is rotating above the water, but with a different set of boundary conditions. In the vertical direction, the kinematic condition is that the change in the surface height $z=\eta(r,\varphi)$ is determined by the vertical flow at the surface such that

$$\frac{\partial\eta}{\partial t}=v_z. \tag{31}$$

However, the other boundary condition at the liquid vapor interface has to do with the transverse stress τ,

$$\tau_{\mathrm{int}}=\left(\mu\frac{\partial v_\varphi}{\partial z}\right)_{\mathrm{liq}}=\left(\mu\frac{\partial v_\varphi}{\partial z}\right)_{\mathrm{gas}}. \tag{32}$$

The boundary condition at the gas–liquid interface can be expressed using a drag coefficient C_D for the atmosphere above the water,

$$\tau_D=\left(\mu\frac{\partial v_\varphi}{\partial z}\right)_{z=\eta}=\frac{1}{2}C_D\rho_{\mathrm{air}}V_{\mathrm{wind}}^2, \tag{33}$$

since it is only in the φ direction that we find the major wind velocity.

As a first approximation, the convectional derivatives are neglected and an approximate solution of the resulting linear system is sought, since the frequencies and velocities of interest are quite small. Oscillatory solutions are sought for the fluid motion due to the wind velocity. A Fourier time transform of all quantities $v_r(\omega)$, $v_\varphi(\omega)$, $v_z(\omega)$, and $p(\omega)$, are taken and it is assumed that everything has a time dependence of $e^{i\omega t}$. It is also assumed that the hurricane has the shape of a vortex flow[22] around the z axis, with a velocity given by

$$v_\varphi = \begin{cases} \Omega r, & r \leqslant a, \\ \Omega a^2/r & r \geqslant a, \end{cases} \tag{34}$$

where the rotational frequency of the hurricane is labeled Ω and a is the effective eye radius. Incorporating the body force due to gravity at the surface, into the linearized Navier–Stokes equations, yields

$$\frac{1}{r}\frac{\partial(r v_r)}{\partial r} + \frac{\partial v_z}{\partial z} = 0, \tag{35}$$

the radial component of the momentum equation

$$i\omega v_r = -\frac{1}{\rho}\frac{\partial p}{\partial r} - g\frac{\partial \eta}{\partial r} + \nu\left(\frac{\partial^2 v_r}{\partial r^2} + \frac{1}{r}\frac{\partial v_r}{\partial r} + \frac{\partial^2 v_r}{\partial z^2} - \frac{v_r^2}{r}\right), \tag{36}$$

the azimuthal component of the momentum equation

$$i\omega v_\varphi = \nu\left(\frac{\partial^2 v_\varphi}{\partial r^2} + \frac{1}{r}\frac{\partial v_\varphi}{\partial r} + \frac{\partial^2 v_\varphi}{\partial z^2} - \frac{v_\varphi^2}{r}\right), \tag{37}$$

and the axial component of the momentum equation

$$i\omega v_z = -\frac{1}{\rho}\frac{\partial p}{\partial z} - g\frac{\partial \eta}{\partial z} + \nu\left(\frac{\partial^2 v_z}{\partial r^2} + \frac{1}{r}\frac{\partial v_z}{\partial r} + \frac{\partial^2 v_z}{\partial z^2}\right). \tag{38}$$

Introducing the vertical boundary condition, yields

$$i\omega\eta = v_z, \tag{39}$$

so that

$$\frac{\partial \eta}{\partial r} = \frac{1}{i\omega}\frac{\partial v_z}{\partial r} \tag{40}$$

and

$$\frac{\partial \eta}{\partial z} = \frac{1}{i\omega}\frac{\partial v_z}{\partial z}. \tag{41}$$

Now, seeking an approximate solution, an assumption is made about the factor structure of the solutions to derive separable ordinary differential equations. That is,

$$v_r(r,\varphi,z,\omega) = J(r,\omega)F(z,\omega), \tag{42}$$

$$v_z(r,\varphi,z,\omega) = H(r,\omega)F(z,\omega), \tag{43}$$

$$v_\varphi(r,\varphi,z,\omega) = G(r,\omega)F(z,\omega), \tag{44}$$

$$p + \rho g z = L(r,\omega)F(z,\omega), \tag{45}$$

which implies that all four functions have the same z dependence.

The continuity equation is found to be separable,

$$\frac{1}{r}\frac{\partial(r v_r)}{\partial r} + \frac{\partial v_z}{\partial z} = 0 = \frac{1}{r}\frac{\partial(rJ)}{\partial r}F + H\frac{\partial F}{\partial z},$$

and adopting β as a separation constant,

$$\frac{1}{H(r)}\frac{\partial(rJ(r))}{\partial r} = -\frac{1}{F(z)}\frac{dF}{\partial z} = -\beta. \tag{46}$$

The equation for a dimensionless $F(z)$ can be solved immediately

$$F(z) = F_0 e^{\beta z}, \tag{47}$$

which vanishes as $z \to -\infty$. At this stage, our consideration is effectively limited to an infinitely deep ocean. The following is then obtained:

$$H(r) = -\frac{1}{\beta}\left[\frac{\partial J}{\partial r} + \frac{J(r)}{r}\right]. \tag{48}$$

Now because $F(z)$ is a factor in all equations, set $F_0 = 1$ and factor it out of all equations at the surface to obtain

$$i\omega J = -\frac{1}{\rho}\frac{dL}{dr} - \frac{g}{i\omega}\frac{\partial H}{\partial r} + \nu\left[\frac{\partial^2 J}{\partial r^2} + \frac{1}{r}\frac{\partial J}{\partial r} + \left(\beta^2 - \frac{1}{r^2}\right)J\right], \tag{49}$$

$$i\omega G = \nu\left[\frac{\partial^2 G}{\partial r^2} + \frac{1}{r}\frac{\partial G}{\partial r} + \left(\beta^2 - \frac{1}{r^2}\right)G\right], \tag{50}$$

$$i\omega H = -\frac{\beta}{\rho}L - \frac{g}{i\omega}\beta H + \nu\left[\frac{\partial^2 H}{\partial r^2} + \frac{1}{r}\frac{\partial H}{\partial r} + \left(\beta^2 - \frac{1}{r^2}\right)H\right]. \tag{51}$$

The boundary condition for the horizontal stress is

$$\frac{\partial v_\varphi}{\partial z} = \frac{\tau_D}{\mu} = \frac{1}{\mu}\frac{1}{2}C_D\rho_{\mathrm{air}}V_{\mathrm{wind}}^2, \quad z = \eta. \tag{52}$$

Since $v_\varphi = G(r)F(z)$,

$$G(z)\beta e^{\beta\eta} = \beta G(z) = \frac{\tau_D}{\mu} = \frac{1}{2\mu}C_D\rho_{\mathrm{air}}V_{\mathrm{wind}}^2, \tag{53}$$

assuming that the displacement of the surface is small, $\beta\eta < 1$.

The boundary condition at the surface may be rewritten as

$$\beta G(r) = \frac{1}{2\mu}C_D\rho_{\mathrm{air}}\begin{cases}(\Omega r)^2, & r \leqslant a, \\ (\Omega a^2/r)^2, & r \geqslant a,\end{cases} \tag{54}$$

or

$$\beta G\left(\frac{r}{a}\right) = \frac{1}{2\mu}C_D\rho_{\mathrm{air}}(\Omega a)^2\begin{cases}(r/a)^2, & r/a \leqslant 1, \\ (a/r)^2, & r/a \geqslant 1.\end{cases} \tag{55}$$

So, if $V_{\max} = \Omega a$, including one factor of $V_{\max}$ in the definition of β and the other factor in the definition of $G(r/a)$, since $G(r/a)$ must have units of velocity, yields an expression for β:

$$\beta = \frac{1}{2\mu_{\mathrm{water}}}C_D\rho_{\mathrm{air}}(\Omega a) = \frac{1}{2\mu_{\mathrm{Sea}}}C_D\rho_{\mathrm{air}}V_{\max}. \tag{56}$$

Our solution for $G(r/a)$ can be determined by the Hankel transform $K(u)$ of the first order Bessel function

$$\int K(u)J_1\left(u\frac{r}{a}\right)du = G\left(\frac{r}{a}\right) = V_{\max}\begin{cases}(r/a)^2, & r/a \leqslant 1, \\ (a/r)^2, & r/a \geqslant 1.\end{cases} \tag{57}$$

These conditions determine the value of the separation constant β. In the comparisons with observation the temperature dependence of the viscosities, densities, and velocities near the ocean surface is used for the evaluation of β. There are no adjustable parameters in β.

In the next few steps an approximate frequency dependence is sought and the viscosity, to lowest order, is included to give a broadening to the resonances. For the axial component of velocity at the surface, this yields

$$\left[i\omega + \frac{g\beta}{i\omega} - \nu\beta^2 \right] H(r) = -\frac{\beta}{\rho} L(r) \tag{58}$$

or

$$H(r) = i\frac{\omega\beta}{\rho}\frac{L(r)}{\omega^2 - g\beta + i\nu\beta^2\omega}. \tag{59}$$

Observe the resonance in $H(r,\omega)$ at the frequency

$$\omega = \sqrt{g\beta} \tag{60}$$

or

$$f_\beta = \frac{1}{2\pi}\sqrt{g\beta}. \tag{61}$$

This resonance will not depend on how fast the hurricane is moving but rather on the maximum wind speed of the storm,

$$f_\beta = \frac{1}{2\pi}\left(\frac{gC_D\rho_{\mathrm{air}}V_{\max}}{2\mu_{\mathrm{H_2O}}} \right)^{1/2}. \tag{62}$$

White notes that Blasius developed a drag coefficient for a flat plate as a function of a Reynolds number Re_a, which depends on the disk radius a, in this case, the eyewall radius,

$$C_D = \frac{1.328}{\sqrt{\mathrm{Re}_a}}, \tag{63}$$

where

$$\mathrm{Re}_a = \frac{V_{\max}a}{\upsilon} \tag{64}$$

and υ is the kinematical viscosity of air.

The parameter β thus depends on the maximum velocity of the hurricane $V_{\max}$, the effective eyewall radius a, and the temperature, density, and viscosity of the air and water. All of these parameters are accessible from the National Hurricane Center[23] (NHC) archival data, if the eyewall radius is determined by a fit from the reported external wind fields that surround the hurricane.

VI. COMPARISON OF HURRICANE BONNIE DATA WITH THE CYLINDRICAL SHEAR FLOW MODEL

Using the Fordham Seismic Station, seismic signals were recorded at each hour for most of the movement of hurricane Bonnie in August 1998. Each 1024 points of data were recorded from August 21 at 0900Z to August 30 at 2200Z on each hour at a frequency of 20 Hz using a vertical seismometer and were collected in one large data file using a 23 bit A to D converter. Data on the location, wind fields at various radii, wind speed, and velocity of movement of the storm were collected and recorded from advisories issued by the NHC. The effective eyewall radius a was determined by fitting the observed wind speeds in four quadrants at various distances from the storm as reported by the NHC advisories.

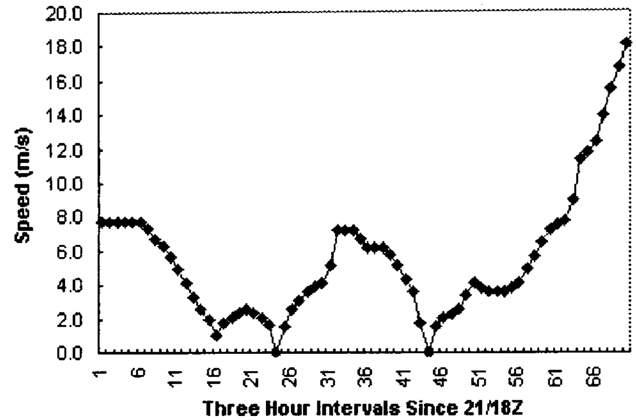

FIG. 1. Speed of Hurricane Bonnie as estimated by the National Hurricane Center at 3 hour intervals since August 21 at 1800Z.

The first step of this study is to construct the velocity of the hurricane. These results are included in Fig. 1. This shows the NHC reported velocity as Bonnie carried out a motion that had the hurricane essentially motionless near a time of reporting an advisory in three different locations. The first two times the storm slowed down and stopped it was far at sea and intensified while motionless over warm water. The third time the storm stopped it had just made landfall on the Carolina coast and turned back to go out to sea again before passing to the north and northeast.

For the following discussion it is necessary to acquaint the reader with graphing conventions followed in the rest of this paper. The frequencies at which Fourier coefficients have been measured are integer multiples of 1/51.25 Hz. This fundamental unit is imposed by our sampling rate and collection time. In all of the following plots of Hurricane Bonnie data, the integral number of such units, which we call frequency index units are plotted. The physical frequency can be obtained by multiplying the frequency index unit by 0.0195 Hz. The time intervals at which power spectrum data are compared with the NHC data are 3 hour intervals which correspond to the time interval between the two different types of advisories issued while a hurricane is monitored. In some references below, the notation 21/18Z is used to designate, August 21, 1998 at 1800 hours Zulu. Occasionally, reference is made to an hour by the designation fd50, which designates the 50th power spectrum recorded by the Fordham seismometer.

In order to get a better idea of whether seismometer data are signals being generated by the hurricane and not New York noise, it is useful to plot in Fig. 2 the total radiated intensity between the 4th and 40th frequency index unit as a function of time and compare it to a theoretically expected intensity from each hurricane location. This frequency range includes all microseisms and should capture the nonzero frequency intensity which is radiated by the hurricane. Along with the observed radiated intensity, Fig. 2 also contains a normalized plot of the inverse squared arc length distance

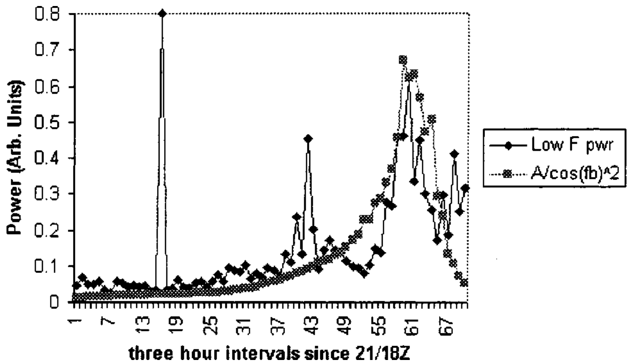

FIG. 2. Low frequency seismometer power (arbitrary units) and the normalized inverse squared distance between Bonnie and Fordham versus 3 hour intervals since August 21 at 1800Z.

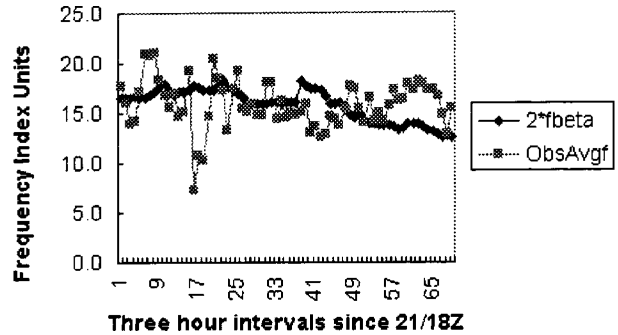

FIG. 3. The observed average frequency and the theoretical double frequency from the cylindrical shear flow theory versus 3 hour intervals since August 21 at 1800Z.

along the surface of the earth from the hurricane to the seismometer site. This inverse squared arc length is labeled $1/\cos(fb)^2$ where fb is the angular separation of the hurricane and Fordham on the surface of the earth. This $A/\cos(fb)^2$ function is scaled to match the received power at the point of closest approach and gives a rough measure of the expected intensity signals generated by the storm. This distance dependence should roughly track the radiated intensity of the microseisms by the hurricane source.

Several features of Fig. 2 require comment. First, the intensity as a function of time and distance is fairly close to the inverse squared arc length distance. This suggests that most of this signal is from the hurricane and not from noise in the vicinity of the seismometer. Second, there are two very anomalous peaks that are much more intense than the other points. In fact, the first point (Interval 16, fd50, 23/15Z) has actually been truncated to make the graphic observable. The actual value is almost 75 times more than the value plotted here. The second peak (Interval 43, fd135, 27/03Z) is the correct value as plotted.

What is happening at these two intensity peaks? Careful correlation with the hurricane location indicates that these two peaks are generated when the hurricane is stationary. The first time Bonnie is at sea and the second peak represents the reversal upon landfall and the return to the sea. The third peak in Fig. 2 is due to the intensity variation as the hurricane reaches its closest point to Fordham and then passes on to the northeast.

Figure 2 gives confidence that measured signals are from the hurricane Bonnie. The next test will be to see if the dominant peaks, essentially the average frequency, of the power spectrum is close to the prediction of $2f_\beta$, which is expected if the kinetic energy is integrated over the circular area of the storm. A positive integrand is expected since the velocity is squared in the cylindrical area of integration. Parameters are chosen to match the temperatures of the south Atlantic and derived other variables from the data on Hurricane Bonnie from the NHC.

Figure 3 plots the observed average frequency and twice the resonant frequency $2f_\beta$ as a function of the advisories issued by the NHC. In these plots the frequency is measured by the frequency index l, the actual value of the frequency is $0.0195\times l$ Hz.

The agreement between the average observed frequency and $2f_\beta$ indicates that the kinetic energy is the contribution to the pressure at the bottom of the ocean even though the hurricane is moving. A small translation of the cylindrical coordinates by a translation velocity v_T does not seem to make much of a difference. Consider the velocity of fluid under a moving hurricane (assumed here in the x direction) the kinetic energy expression will be

$$\tfrac{1}{2}(v_T\mathbf{e}_x+v_r\mathbf{e}_r+v_\varphi\mathbf{e}_\varphi+v_z\mathbf{e}_z)(v_T\mathbf{e}_x+v_r\mathbf{e}_r+v_\varphi\mathbf{e}_\varphi+v_z\mathbf{e}_z) \quad (65)$$

which becomes

$$\tfrac{1}{2}(v_T^2+v_\varphi^2+v_r^2+v_z^2+2v_Tv_r\mathbf{e}_r\cdot\mathbf{e}_x+2v_Tv_\phi\mathbf{e}_\phi\cdot\mathbf{e}_x). \quad (66)$$

The last two terms average out when integrated over ϕ while the first two terms have no time dependence and so make no contribution. The two terms $v_r^2+v_z^2$ both will exhibit the $2f_\beta$ frequency.

So, the remaining question to be answered is what is happening at the points where the hurricane has stopped. The hint can be seen in Fig. 3 at the location of the first peak. The average frequency is almost exactly at f_β. The explanation returns to the Bernoulli equation and the contribution of the gravitational potential energy, which has a resonance at f_β,

$$g\rho\eta(r,\omega)=g\rho\frac{v_z}{i\omega}=\frac{g\rho H(r)}{i\omega}=g\beta\frac{L(r)}{\omega^2-g\beta+i\nu\beta^2\omega}. \quad (67)$$

As noted by LH and discussed above, if such a oscillation moves along the surface as a traveling wave, it does not make a significant contribution to radiated microseisms. However, if there is no translational motion, then an oscillation in the vertical direction will be coherent and give rise to an excitation on the floor at the frequency $\sqrt{g\beta}$. If the storm is motionless, the gravitational potential energy of the surface should be seen in the microseism spectrum.

It is useful to examine the power spectrum as measured by the spectrometer to describe these phenomena. Two different plots of the power spectrum are shown below, the first of these will be 3 hours before the hurricane stops at (Interval 16, fd50, 23/15Z) and will show behavior similar to most hours of microseism production.

The spectrum (fd47,23/12Z) in Fig. 4 is fairly typical for a moving hurricane. There is a dominant peak close to the frequency $2\sqrt{g\beta}$ as well as a number of other smaller peaks

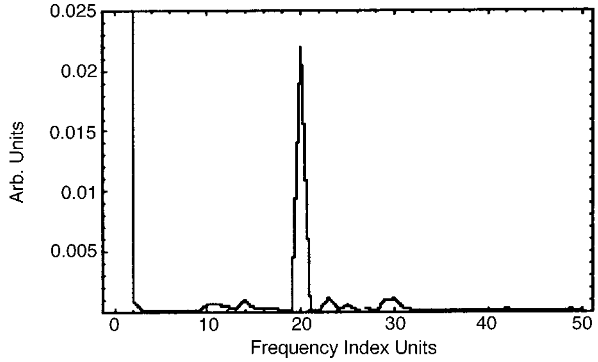

FIG. 4. The microseism power spectrum at the 47th hour of data plotted in frequency index units of 0.195 Hz.

which fluctuate in time. Notice that the maximum vertical scale of this graph is 0.025 arbitrary units, which is typical of the spectrum in this early path of the hurricane. Figure 5 shows the power spectrum for the 50th hour (df50,23/15Z) during which the hurricane was motionless. Notice immediately that the vertical scale here is 4.0, a factor of 160 larger than the previous figure. Note also the significant change in the location of this peak as well as the large increase in intensity. While the much smaller peak in Fig. 4 was very close to $2\sqrt{g\beta}$, the spectrum in Fig. 5 is dominated by the very large peak very close to $\sqrt{g\beta}$. At the hour 50 (fd50, 23/15Z) the frequency of the peak is between 8.75 and 9.0 frequency index units. The calculated value of f_β. is found to be 8.87 units.

At the second intensity peak (fd130, 26/20Z) the peak location is approximately 11 frequency index units and the theoretical value of f_β is about 9. The peak is not quite as large as the case for the 50th hour, but it must be remembered that much of the hurricane was over land when it stopped and moved back onto the sea. A smaller signal from the remaining part of the hurricane over the ocean should be expected.

In Fig. 1 there was a third time in which the NHC reports a zero velocity for Bonnie. This was at (Interval 23, fd75, 24/15Z). A review of a number of measured power spectrum near this time show spectra with f_β peaks dominant at fd70–fd73 and fd79–fd81. None of these lower frequency peaks is as large as observed at fd50. Even though the NHC reports the hurricane having zero velocity in a three hour period, our data would indicate the velocity was slowly changing and was zero before and after the advisory at 24/15Z.

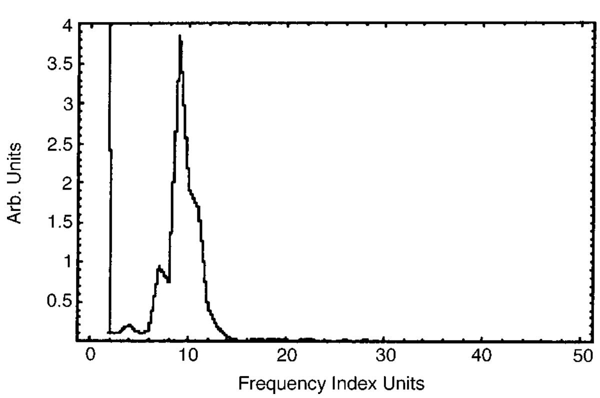

FIG. 5. Microseism power spectrum at the 50th hour plotted versus frequency index units of 0.195 Hz.

A similar analysis of the times around the third peak near Interval 60 in Fig. 5 shows that the spectrum is concentrated at frequencies closer to $2\sqrt{g\beta}$ and there is no shift to a lower frequency during this period. The microseisms generated here appear to arise primarily from the kinetic energy terms in Bernoulli's equation.

The power spectrum at different hours was never exactly the same. Most of the largest peaks are close to the $2\sqrt{g\beta}$ frequency as shown in Fig. 4, although there is some variation with time. The parameters that have been used to calculate β are averages computed over the whole lifetime of the hurricane and the real values must change with time more quickly than indicated by our data. This theory clearly is only a first approximation in which fluctuations are ignored. In spite of this limitation, it appears that this vortex theory captures much of the radiated microseism generation by this hurricane.

VII. EXTENSION OF THE CYLINDRICAL STRESS FLOW MODEL TO MID-LATITUDE CYCLONES

A second study was carried out with the Fordham Seismic Station during the passage of a strong Nor'easter which moved up the East Coast in January 1998. Seismic data were gathered when the storm was close to Fordham so the storm would dominate the seismic data. The data were collected for January 21 and 22 and average frequencies of the microseisms were tabulated hourly for this time period. A series of satellite images and detailed surface weather maps[24] were used to map the location of the storm and estimate its speed, size, and pressure.

The preceding theory for hurricanes was based on the assumption that the storm structure resembled a vortex with an eyewall parameter a and a maximum velocity $V_{\max}$. The structure of the mid-latitude cyclone is quite different. In the next few paragraphs the cylindrical stress–flow model is adapted to this atmospheric structure.

The striking structure of mid-latitude cyclones as represented by our nor'easter is that the isobars are approximately circular and that the pressure gradient is radial and essentially constant. A balancing of the Coriolis force and the pressure gradient forces induces the main winds to be predominantly azimuthal.

The equations of motion for the air above the sea are derived in a cylindrical coordinate system that rotates about the local zenith with a Coriolis rotation frequency Ω_c. Letting v_r and v_ϕ be the radial and azimuthal velocities of the air at the bottom of the cyclone and at the surface of the water, yields the following equations (without viscosity):

$$\frac{\partial v_r}{\partial t} - 2\Omega_c v_\phi - \frac{v_\phi^2}{r} = \Omega_c^2 r - \frac{1}{\rho_{\mathrm{air}}}\frac{\partial P}{\partial r}, \tag{68}$$

$$\frac{\partial v_\phi}{\partial t} + 2\Omega_c v_r + \frac{v_r v_\phi}{r} = 0. \tag{69}$$

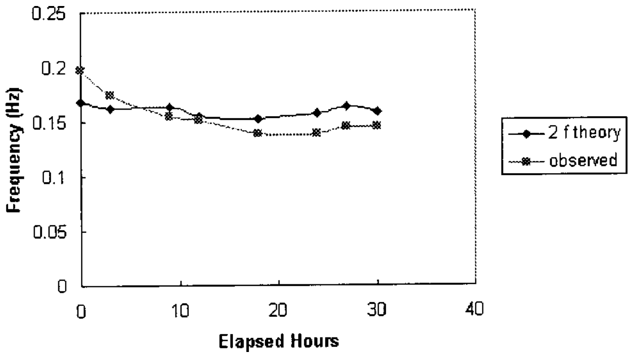

FIG. 6. Theoretical and observed 2f frequencies for the mid-latitude cyclone microseisms.

To find the steady state solution, set the derivatives on the left-hand side to zero and solve the remaining equations. This implies that $v_r=0$ and that v_ϕ depends on r in a simple fashion. In order to write this, impose the assumption that the radial pressure gradient of the pressure is constant. It may then be evaluated by measuring the pressure difference ΔP between the outermost isobar and the center, and the radius R_c of the cyclone between these same two points. Defining the maximum azimuthal air velocity

$$(v_\phi)_{\max}=\frac{1}{4\Omega_c}\frac{\Delta P}{\rho_{\text{air}}R_c}, \tag{70}$$

and a characteristic length for the velocity variation

$$a=\frac{1}{\Omega_c^2}\frac{\Delta P}{\rho_{\text{air}}R_c}, \tag{71}$$

yields the steady state solution for the azimuthal velocity

$$v_\phi=4(v_\phi)_{\max}\sqrt{\frac{r}{a}}\left(1-\sqrt{\frac{r}{a}}\right). \tag{72}$$

Inserting these into the boundary condition between the air and water and using the Blasius drag coefficient results in

$$\beta G(z)=\frac{1.328\rho_{\text{air}}\sqrt{\nu_{\text{air}}}(4(v_\phi)_{\max})}{2\mu\sqrt{R_c(v_\phi)_{\max}}}\times 4(v_\phi)_{\max}\frac{r}{a}\left(1-\sqrt{\frac{r}{a}}\right)^2. \tag{73}$$

Following factorization, and the same process as before, we find that β is given by

$$\beta=\frac{1.328\rho_{\text{air}}\sqrt{\nu_{\text{air}}}(4(v_\phi)_{\max})}{2\mu\sqrt{R_c(v_\phi)_{\max}}}. \tag{74}$$

By combining appropriate temperatures, densities, viscosities and measured pressure differences ΔP and average radii R_c from the surface weather maps,[24] the predicted stress–flow frequencies f_β are calculated for this storm.

The comparison of the average measured microseism frequency and the double frequency $2f_\beta$ were tabulated and the results are shown in Fig. 6. As can be seen, the difference between the theoretical and observed frequencies varies from 3% to 10%. Again, there have been no adjustable parameters in any of the theoretical calculations.

VIII. COMPARISONS WITH OTHER OBSERVATIONS

This study was originally stimulated by the work of Tabulevich and it would be gratifying to extend its predictions against her carefully gathered data. The data supplied for a cyclone observed crossing the Caspian Sea in 1956 minimally provides the required data, including a sketch of isobars. Inserting best guesses for values needed to calculate $2f_\beta$ for a mid-latitude cyclone, a 10% to 25% difference is found between experimental and theoretical periods. Similar sets of observations over Lake Baikal and the Okhotsky Sea were more ambiguous. Otherwise, the theory generated here satisfies most of Tabulevich's observations concerning the essential role of a cyclonic storm structure in generating microseisms.

While the main purpose of this paper has been to explain microseisms radiated from cyclonic storms, it is worthwhile to address the question of the equilibrium microseisms spectrum as measured from the sea floor. This question of the "climatology" of microseisms has been studied carefully by Webb[10] and compared with bottom measured spectra measured at different sites in the Pacific. The fundamental premise underlying Webb's treatment is that acoustic waves generated by gravity wave pairs are responsible for the equilibrium microseism spectrum observed in measurements. As a model of the sea for this calculation Webb used a gravity wave height versus frequency distribution suggested by Pierson and Moskowitz.[25] Webb carries out a careful and thorough study of the distribution of acoustic waves generated by gravity wave interactions and their approach to equilibrium.

From the perspective postulated by the current authors, the spectrum should be a direct consequence of the surface wave distribution as expressed through Eq. (13). A calculation of the frequency dependent pressure at the bottom of the sea through the Bernoulli principle was carried out in direct comparison with the theory and experiment of Webb.

If the consequence of the Bernoulli principle is recognized and the contribution of the non-linearly generated acoustic waves is ignored, the equilibrium spectrum should be a direct reflection of the equilibrium wave height distribution. The sea-floor pressure fluctuations $\Delta p(\omega)$ at a frequency ω should be given by

$$\Delta p(\omega)=\frac{1}{2}\rho\int v(x,y,\eta,t,t)^2 e^{i\omega t}\,dt, \tag{75}$$

where $v(x,y,\eta,t,t)$ is the surface gravity wave velocity at the surface. The equilibrium distribution for this velocity was calculated using the same wave height distribution $H(\omega)$ as discussed by Webb

$$v(x,y,\eta,\Delta t)=\frac{1}{2}\int\frac{d\omega}{2\pi}\omega H(\omega)e^{-i\omega t}. \tag{76}$$

Approximate calculations of the pressure power spectrum for this wave distribution as normalized by Webb and the direct calculation of the pressure power spectrum was carried out and the comparison is Fig. 7 where the two thin lines are digitized graphs from Webb of experimental data in the Pacific, the next thicker line is Webb's calculation for winds of 10 m/s based on acoustic waves, and the broadest line is the

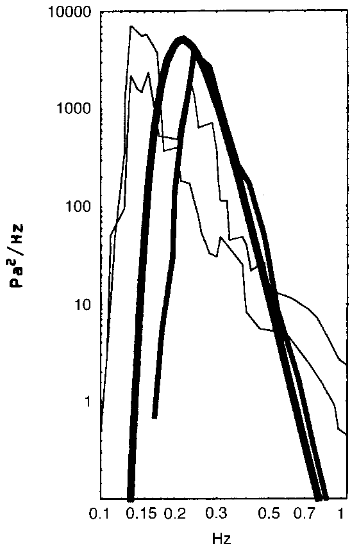

FIG. 7. Comparison of equilibrium microseism spectrum: (thin lines) observations in Pacific, (middle thickness) spectrum calculated by Webb, (heaviest line) spectrum from direct Bernoulli principle.

direct Bernoulli spectrum based on the same Pierson and Moskowitz spectrum for a steady wind of 10 m/s. It should be noted that both of the theoretical predictions are at higher frequencies than the observations, but that the Bernoulli result extends to lower frequencies than the nonlinear results of Webb.

The detailed microseism and wave spectrum data collected by Kibblewhite and Ewans[11] was originally interpreted as evidence of the nonlinear interaction of surface gravity waves to create acoustic waves. The data can be seen to support the Bernoulli principle as well. The time course of microseism events are much better explained by the approach and passing of the anticyclone with the maximum occurring at the point of closest approach of the storm center. This behavior should parallel the observations of Hurricane Bonnie in an earlier section of this paper. Kibblewhite and Ewans also present a log–log plot of a very large data set of pressure fluctuations at a given frequency versus the wave amplitude at the same frequency. Given the uncertainty that the wave amplitudes are not measured near the center of the cyclonic storm, the equations above for the pressure at a given frequency due to the Bernoulli principle immediately give rise to a slope of 2 on the log–log plot. The width of the scatter on this plot may be understood in terms of the scatter of the frequencies

$$\ln(\Delta p(\omega)) = \ln(\tfrac{1}{2}\rho\omega^2) + 2\ln(H(\omega)). \tag{77}$$

A further application of the Bernoulli principle for sea bottom pressure is suggested by the intriguing study of microseisms under the ice covered Beaufort Sea.[9] Relatively sharp resonances are observed in a very quiet environment under the ice layer. In this paper it was assumed by Webb that an acoustic wave guide theory could achieve similar resonances by assuming standing wave resonances in the wave guide for a particular depth and boundary condition. However, as expressed in this reference, the resonant conditions (depth and boundary conditions) do not closely correspond to the conditions on the depth and sea-floor covering of the Beaufort Sea. Furthermore, since the floor of the sea is very fluid and covered with a deep layer of sediment, it would be expected that the resonances would have been wider due to acoustic losses at both boundaries.

An alternative theory for these sharp resonances is suggested by the presence of the ice layer and the Bernoulli principle. If there are very low frequency shear waves excited along the length of the ice pack section over the bottom detectors, these waves should have an influence on the floor pressure due both to the potential and kinetic energy of such waves. If the length of distance between major cracks or discontinuities of the ice island is L and the velocity of sound in the ice is c, then the low lying modes (standing wave frequencies) of the ice layer would be given by $f=(c/L)n$ where $n=1,2,3,4,5,\ldots$. If these frequencies are present in the Bernoulli expression for the bottom pressure, the effects of the potential energy f and kinetic energy $2f$ of these surface modes should appear as the following multiples of the lowest mode: 1, 2, 3, 4, 5, 6, 8, 10, 12, 14. The even frequency peaks should be larger than the odd peaks should they represent both a potential and kinetic energy contribution. The odd peaks will represent only the potential energy. If the lowest mode is chosen to be the peak at 0.077 Hz, then all of these modes are clearly seen except for 3, 5, and 8,10. The location for the third and fifth frequency multiple would occur on the sides of large and wide peaks for 2 and 4. Near the required locations are slight shoulders which could be these modes potential energy modes. Since these modes represent a contribution from the potential energy and all even frequencies are also from the kinetic energy contribution, it is likely to be harder to observe these two odd frequencies. The frequencies at 8 and 10 are not clearly resolved in the data, but there is a broad peak at 9 times the base frequency which could be an unresolved combination of these two peaks. The other peaks do correspond well with the remaining multiples. Taking reasonable values for the velocity of sound in ice[26] obtained from the Army Cold Weather Laboratory, the length of the ice island would be about 10 miles.

Finally, the application of the mid-latitude cyclone cylindrical stress–flow model of this paper to the time evolution of microseisms observed on the bottom of the Pacific[8] in February 1983 as a presumably, cyclonic storm passed over or near to the detectors would offer a further test of these ideas.

IX. CONCLUSION AND NEED FOR FURTHER STUDY

The cylindrical stress–flow model for the generation of microseisms developed here has displayed much success in predicting the average frequencies of microseisms and their dependence on environmental variables. At the same time there are many details that have been left unexamined in this paper. The average or dominant frequencies were well predicted, but the other peaks which appear in microseism power spectra have not been examined. The fluctuations from the mean motion which was assumed have been ignored as has any explanation of the lifetime broadening of the microseisms themselves. Experimentally microseisms appear as short wave trains less than 10 cycles in duration. Neither the wave train length or the arrival statistics of microseisms have been explained yet.

The ideas in this paper do not argue directly against the nonlinear generation of acoustic waves by gravity waves which has come to dominate the theoretical treatments of microseisms. The objective of this paper is to argue that the direct application of the Bernoulli principle can explain much of the observed phenomena by itself. Further study should lead to assessment of the roles of these two distinct mechanisms.

The distinction between measuring pressure variations at a point on the sea floor (at the foot of a column of water) and the conditions necessary to detect a radiated seismic signal at a distant seismometer has been delineated. This distinction should eliminate the need to search for reflected and/or standing waves over the sea floor detectors since coherence over a wide area is not required.

Most of the study in this paper has been directed toward radiated microseisms which can only be detected with seismometers. These same effects should be evident as infrasound and an effort at detecting such signals near large bodies of water as storms pass over would be an important further test of these ideas.

ACKNOWLEDGMENTS

The principal author (S.B.) would like to acknowledge the hospitality of the Fordham Physics Department during several visits. Finally, without the readily accessible archives and staff of the National Hurricane Center and the National Climatic Data Center, none of this work would have been possible. The help of Dr. Donald G. Albert of the Army Cold Weather Research Center on velocities of ice is gratefully acknowledged.

[1] V. N. Tabulevich, *Microseisms and Infrasound Waves* (Springer, Verlag, 1992).
[2] J. E. Ramirez, ''An experimental investigation of the nature and origin of microseisms at St. Louis, Missouri, Parts One and Two,'' Bull. Seismol. Soc. Am. **30**, 35–84 (1940); **30**, 139–174 (1940).
[3] R. K. Cessaro and W. W. Chan, ''Wide-angle triangulation array study of simultaneous primary microseism sources,'' J. Geophys. Res., [Oceans] **94**, 15555–15563 (1989).
[4] M. S. Longuet-Higgins, ''Theory of the origin of microseisms,'' Philos. Trans. R. Soc. London, Ser. A **243**, 1–35 (1950).
[5] A. C. Kibblewhite and C. Y. Wu, ''The generation of infrasonic ambient noise in the ocean by nonlinear interactions of ocean surface waves,'' J. Acoust. Soc. Am. **85**, 1935–1945 (1989); ''A reexamination of the role wave–wave interactions in ocean noise generation,'' *ibid.* **85**, 1946–1957 (1989); A. C. Kibblewhite and C. Y. Wu, ''The theoretical description of wave-wave interactions as a noise source in the ocean,'' *ibid.* **89**, 2241–2252 (1991).
[6] B. Hughes, ''Estimates of underwater sound (and infrasound) produced by non-linearly interacting ocean waves,'' J. Acoust. Soc. Am. **60**, 1032–1039 (1976).
[7] R. H. Nichols, ''Infrasonic ambient ocean noise measurements: Eleuthera,'' J. Acoust. Soc. Am. **69**, 974–981 (1981).
[8] S. C. Webb and C. S. Cox, ''Observations and modeling of seafloor microseisms,'' J. Geophys. Res., [Oceans] **91**, 7343–7358 (1986).
[9] S. C. Webb and A. Schultz, ''Very low frequency ambient noise at the seafloor under the Beaufort Sea icecap,'' J. Acoust. Soc. Am. **91**, 1429–1438 (1992).
[10] S. C. Webb, ''The equilibrium oceanic microseism spectrum,'' J. Acoust. Soc. Am. **92**, 2141–2157 (1992).
[11] A. C. Kibblewhite and K. C. Ewans, ''Wave-wave interactions, microseisms, and infrasonic ambient noise in the ocean,'' J. Acoust. Soc. Am. **78**, 981–994 (1985).
[12] M. V. Trevorrow, T. Yamamoto, A. Turgut, and D. Goodman, ''Measurements of ambient seabed seismic levels below 1.0 Hz on the shallow eastern US continental shelf,'' J. Acoust. Soc. Am. **86**, 2318–2327 (1989); D. Goodman, T. Yamamoto, M. Trevorrow, C. Abbott, A. Turgut, M. Badiey, and K. Ando, ''Directional spectra observations of seafloor microseisms from an ocean bottom seismometer array,'' *ibid.* **86**, 2309–2317 (1989).
[13] G. H. Sutton and N. Barstow, ''Ocean bottom microseisms from a distant supertyphoon,'' Geophys. Res. Lett. **23**, 499–502 (1996).
[14] B. Kinsman, *Wind Waves* (Prentice-Hall, Englewood Cliffs, NJ, 1965).
[15] O. M. Phillips, ''On the generation of waves by turbulent wind,'' J. Fluid Mech. **2**, 417–445 (1957).
[16] J. W. Miles, ''On the generation of surface waves by shear flows,'' J. Fluid Mech. **3**, 185–204 (1957).
[17] C. C. Mei, *The Applied Dynamics of Ocean Surface Waves* (World Scientific, Singapore, 1989).
[18] P. M. Morse and H. Feshbach, *Methods of Theoretical Physics* (McGraw-Hill, New York, 1953), p. 809.
[19] B. Kinsman, *Wind Waves* (Prentice Hall, Englewood Cliffs, NJ, 1965), p. 543.
[20] F. M. White, *Viscous Fluid Flow* (McGraw-Hill, New York, 1974).
[21] F. M. White, *Viscous Fluid Flow* (McGraw-Hill, New York, 1974), pp. 165 and 265.
[22] P. M. Morse and H. Feshbach, *Methods of Theoretical Physics* (McGraw-Hill, New York, 1953), p. 158.
[23] National Hurricane Center, http://www.nhc.noaa.gov
[24] National Climatic Data Center, http://www.ncdc.noaa.gov
[25] W. J. Pierson and L. Moskowitz, ''A proposed spectral form for fully developed wind seas based on the similarity theory of S. A. Kitaigorodskii,'' J. Geophys. Res. **69**, 5181–5190 (1964).
[26] Army Cold Weather Research Center, http:/www.crrel.usace.army.mil